Journal of Quantitative Spectroscopy & Radiative Transfer 131 (2013) 34–42

Contents lists available at ScienceDirect

Journal of Quantitative Spectroscopy & Radiative Transfer

journal homepage: www.elsevier.com/locate/jqsrt

DNA detection assay based on fluorescence quenching of rhodamine B by gold nanoparticles: The optical mechanisms

T.E. Pylaev [a], E.K. Volkova [b], V.I. Kochubey [b], V.A. Bogatyrev [a,b], N.G. Khlebtsov [a,b,*]

[a] Institute of Biochemistry and Physiology of Plants and Microorganisms, RAS, 13 Prospekt Entuziastov, Saratov 410049, Russian Federation
[b] Saratov State University, 83 Ulitsa Astrakhanskaya, Saratov 410012, Russian Federation

ARTICLE INFO

Article history:
Received 11 December 2012
Received in revised form
19 April 2013
Accepted 23 April 2013
Available online 1 May 2013

Keywords:
Gold nanoparticles
DNA detection
Fluorescence quenching and enhancement
Rhodamine B

ABSTRACT

The different ability of single- and double-stranded oligonucleotides to stabilize gold nanoparticles (GNPs) in solution has recently been used to design several label-free hybridization assays on the basis of optical changes associated with GNP aggregation. DNA hybridization can be detected through changes in dye fluorescence quenching by GNPs. Here we examine the mechanisms behind a fluorescent DNA assay for model systems containing DNA oligonucleotides, 15-nm GNPs, and Rhodamine B (RB). There was a direct correlation between complete disappearance of fluorescence and complete adsorption of all RB molecules on nonaggregated GNPs, as revealed by an analysis of the colloids' supernatant liquids. We show that both the inner filter effect and the quenching of the dye owing to its adsorption on GNPs contribute to the observed changes in fluorescence intensity. Therefore, both factors should be properly adjusted to optimize the assay sensitivity. In particular, the low detection limit of the fluorescent DNA assay lies in the range 30–100 pM, which is close to the data reported previously for colorimetric and dynamic light scattering DNA assays.

1. Introduction

The conventional strategy for nucleic acid detection is based on the polymerase chain reaction (PCR) [1], which allows quantitative DNA determination with high specificity, sensitivity, and efficiency and with low contamination risk [2]. Despite its almost routine applications, the PCR method requires special reagents and cost-effective equipment. Therefore, in certain circumstances (e.g., in warfare or under field conditions), it is desirable to have a rapid and simple qualitative test for primary DNA detection to compete with precise PCR analysis. Colloidal gold nanoparticles (GNPs) form a new platform for colorimetric DNA detection [3,4]. The change in solution color and the plasmon resonance shift that occur owing to particle aggregation are used in various tests for DNA detection [5–9]. The dynamic light scattering detection of DNA has been proven to be more sensitive than the usual spectrophotometry [10,11]. Fluorescent techniques have also been implemented for DNA detection by using fluorophore-labeled oligonucleotide probes attached to GNPs by covalent chemical modification [12] or by physical adsorption [13].

Recently, a new method has been proposed for sensitive quantitative label-free DNA detection by using GNPs and RB as a fluorophore [14]. In this method, RB fluorescence is quenched by GNPs that are stabilized by single-stranded DNA (ssDNA) molecules (Fig. 1). Addition of a complementary DNA (cDNA) target results in hybridization of probes and targets in the formation of double-stranded DNA (dsDNA) duplexes, which cannot stabilize GNPs in salt environment, thus causing their aggregation. As a result, the hybridization reaction is observed as an increase in fluorescence intensity (Fig. 1). It is evident that

* Corresponding author at: Institute of Biochemistry and Physiology of Plants and Microorganisms, RAS, 13 Prospekt Entuziastov, Saratov 410049, Russian Federation. Tel.: +7 845 2 970403.
E-mail address: khlebtsov@ibppm.sgu.ru (N.G. Khlebtsov).

0022-4073/$ - see front matter © 2013 Elsevier Ltd. All rights reserved.
http://dx.doi.org/10.1016/j.jqsrt.2013.04.026

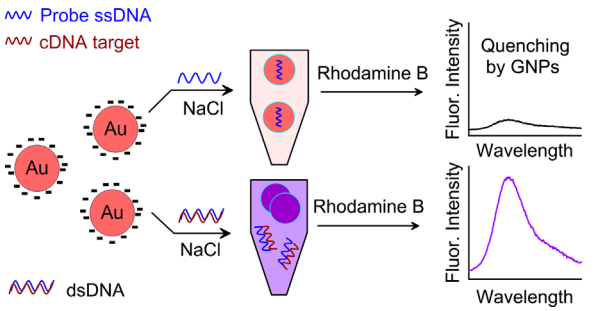

Fig. 1. Schematic representation of the fluorescent method for differentiation between ssDNA and dsDNA by using citrate-stabilized GNPs and the fluorescent dye RB. cDNA is a complementary target DNA to the probe ssDNA.

the principle of the fluorescence assay is similar to that of the previously reported colorimetric and fluorescence assays [10,13,15,16], as all methods utilize the differentiation between the abilities of ssDNA and dsDNA to stabilize GNPs in a salt environment. The possible physicochemical mechanisms behind this differentiation were discussed by Li and Rothberg [15,16].

It is useful to discuss shortly the surface plasmon resonance (SPR) concept underlying the DNA assay being considered. In our case, both the exciting (520 nm) and the emitted (575 nm) light wavelengths lie within the SPR band of individual 15-nm GNPs. In general, interactions of a dye molecule with the SPR particle can be enhanced or quenched [17–20]. The enhancement of fluorescence owing to the plasmonic particle is related to the local field near the particle and is closely related to the well-known electromagnetic contribution to surface-enhanced Raman scattering (SERS) [21–23]. In a first approximation, the electromagnetic enhancement of the SERS scales as $|E|^2$, thus giving rise to a giant amplification of SERS spectra at sites known as "hot spots" [24,25]. In terms of a two-staged model [20,26], the enhanced local SPR field results in an enhanced fluorescence of a dye molecule located near a plasmonic particle at the first stage. At the second stage, the fluorescence light with an increased quantum yield is radiated to its environment (radiative decay loss). On the other hand, when the gap between the particle and the dye molecule is sufficiently small, the major portion of emitted energy will dissipate by the metal particle. These phenomena are more prominent for particle clusters in which the electromagnetic "hot spots" arise near small gaps between the metal surfaces [23,24]. A very simple example is a dimer of plasmonic particles [20,27]. For obtaining maximal fluorescence, the emitting molecule should be placed at an optimal distance from the "hot spot." Although this distance can be controlled with a nanometer accuracy [28], metallic colloids demonstrate quenching rather than enhancement in typical experiments [19]. An additional complicating factor is the strong dependence of the SPR band on particle clustering [29,30], which results in strong deviations in the absorption and scattering spectra of colloids even in the simplest case of dimers [31,32]. Specifically, aggregated colloids exhibit red-shifted and greatly broadened spectra [29,33]. Clearly, the aggregation can cause strong deviations in SPR quenching and enhancement owing to the appearance of new "hot spots" and owing to their spectral movement to red.

In addition to the enhancement and quenching phenomena, SPR colloids exhibit a more trivial yet important mechanism, which can greatly alter the measured fluorescence signals. To simplify the question, let us consider a single dye molecule located right in the center of a cuvette filled with a colloid. Owing to the SPR absorption and scattering bands, the colloid acts as a selective filter. Therefore, the incident (exciting) light will be attenuated after traveling a pass of $l/2$ in accordance with Bouguer's law, $I(\lambda_{em})\exp[-NC(\lambda_{exit})(l/2)]$. Here, N is the particle number concentration, and C_{ext} is the extinction (absorption +scattering) cross-section. For an ideal measuring scheme with a zero-view detector, we will record not the fluorescence intensity $I(\lambda_{em})$ but the following quantity [34]: $I(\lambda_{em})\exp\{-N[C(\lambda_{exit})+C(\lambda_{emit})](l/2)\}$. In the literature, such a selective distortion of the measured fluorescence is called the "inner field effect." Again, it is clear that for plasmonic systems, this effect can greatly affect the measured responses in both aggregated and nonaggregated colloids.

The optical mechanisms underlying the aggregation-induced increase in fluorescence intensity may be as follows [14]. For aggregated particles, the total surface available for adsorption of RB is reduced, thus resulting in an increase in the concentration of free RB molecules and in a corresponding increase in fluorescence intensity. The second factor is known as the above discussed inner filter effect [34].

In our case (Fig. 1), the main contribution to the inner filter effect comes from the selective absorption by isolated or aggregated GNPs. In particular, for aggregated GNPs, the absorption at 520 nm decreases and the intensity of the exciting light increases correspondingly. In addition, the absorption of emitted light, traveling from the exciting point to the detector, diminishes. Eventually, the recorded fluorescence intensity of RB can be higher than that in the case of isolated GNPs.

Although these possibilities were noted by Zhang et al. [14], it remained unclear which of these possibilities (or both) constituted the physical mechanism behind the GNP-based fluorescence test. In this work, we investigate the GNP quenching and the inner filter factors in detail to show that both mechanisms are involved in the increase in overall fluorescence intensity recorded after hybridization of the probe and target ssDNA. In addition, we evaluate the detection limit for the target cDNA, which is close to that for the colorimetric and light scattering assays [11].

2. Experimental details

2.1. Reagents

All 21-mer synthetic ssDNAs, corresponding to portions of the human immunodeficiency virus type 1 (HIV-1) U5 long terminal repeat (LTR) sequence, were purchased from Syntol (Russia). Their base sequences are as follows: probe DNA sequence, 5′-ATGTGGAAAATCTCTAGCAGT-3′; target DNA sequence, 5′-ACTGCTAGAGATTTTCCACAT-3′; and the

noncomplementary DNA target sequence was similar to the probe DNA sequence.

To fabricate GNPs, we used the following reagents: tetrachloroauric acid, $HAuCl_4$ (Alfa Aesar, USA); sodium citrate, $Na_3C_6H_5O_7 \cdot 2H_2O$ (Sigma, USA) and Milli-Q water. To ensure hybridization conditions, we used Tris, $C_4H_{11}NO_3$ (Helicon, Russia); HCl, and NaCl (Reachim, Russia); phosphate buffer in tablets (PB; pH 7.4), 0.01 M (Biolot, Russia); EDTA (Serva, Germany). Rhodamine B (Soyuzreaktiv, Russia) served as a fluorescent dye. TE buffer (pH 7.4) consisted of 10 mM Tris–HCl and 1 mM EDTA. The hybridization buffer (HB; pH 7.4) consisted of 10 mM Tris–HCl, 1 mM EDTA, and 50 mM NaCl. The detection buffer (PBS) consisted of 10 mM PB and 0.3 M NaCl. All solutions were stored at 4 °C before use.

2.2. Fabrication of nanoparticles

GNPs of 15-nm diameter were fabricated by reducing $HAuCl_4$ with sodium citrate by the method of Frens [35], with minor modifications as described by Grabar et al. [36]. Briefly, 25 mL of 38.8 mM sodium citrate was added quickly to boiled 250 mL of a 1 mM water solution of $HAuCl_4$, resulting in a change in solution color from pale yellow to deep red. The average particle size can be tuned by varying the amount of added sodium citrate as described in Ref. [37]. Fig. 2 shows a typical TEM image of 15-nm gold particles and a corresponding size-distribution histogram. According to the TEM analysis, the average particle diameter was 15.9 ± 1.4 nm.

2.3. Measurements

Extinction spectra were recorded with a Specord BS-250 and a Specord S-300 VIS spectrophotometer (Analytik Jena, Germany). Fluorescent spectra were recorded with a Perkin-Elmer LS-55 (Perkin-Elmer, USA) and an Avantes AvaSpec-2048 (Avantes BV, Netherlands) spectrofluorimeters by setting the excitation wavelength at 520 nm and recording the emission intensities at wavelengths ranging from 540 to 650 nm. Throughout the study, the maximal fluorescence intensities were measured at 575 nm. The GNP average diameter was controlled with a Libra-120 transmission electron microscope (Carl Zeiss, Germany) and with a Zeta sizer Nano ZS dynamic light scattering instrument (Malvern, UK).

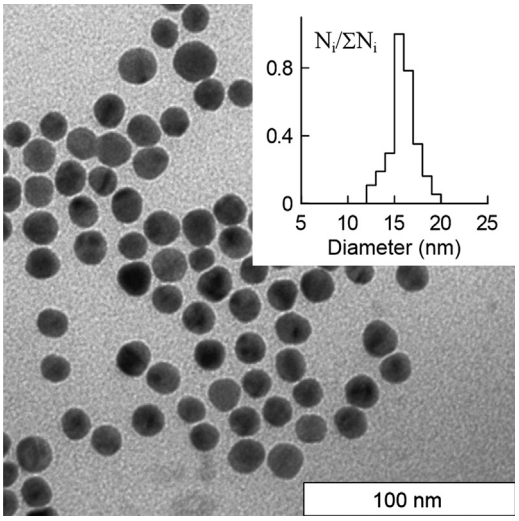

Fig. 2. TEM image of GNPs obtained with a Libra-120 (Carl Zeiss) electron microscope. The inset shows a number–size distribution histogram. Average particle diameter, 15.9 ± 1.4 nm.

3. Results and discussion

3.1. Influence of ssDNA molecules and NaCl from the hybridization buffer on RB fluorescence

Before investigation of the quenching of RB molecules by GNPs, we estimated whether the components of the reaction mixture, namely ssDNA, NaCl from the hybridization buffer, and low-molecular weight components of the GNP supernatant liquid, can influence RB fluorescence. To examine ssDNA effects, we prepared the following three solutions: a reference aqueous RB solution and two aqueous RB solutions containing 300 nM and 1 μM of probe ssDNA. For each solution, the RB concentration was constant and equal to 1.5 μM [14]. The fluorescence spectra were measured for all three samples. It was found that the maximal fluorescence intensities at 575 nm for the ssDNA-containing solutions were lower than that for the reference solution by 0.2–0.5% only (Table 1). Thus, the addition of ssDNA to the RB solution changes fluorescence intensity negligibly and does not affect the fluorescence test.

To investigate the influence of NaCl and the GNP supernatant liquid on RB fluorescence, we prepared an aqueous RB solution, RB in an NaCl solution (final concentration of the detection buffer, 86 mM), and RB dissolved in the supernatant liquid obtained after centrifugation of GNPs. The optimal concentration of NaCl (86 mM) for the maximal fluorescence response was found by Zhang et al. [14] and was confirmed in our experiments.

As shown in Fig. 3, the fluorescence intensity of RB in the salt solution was somewhat higher than the intensity for the aqueous RB solution. This result was reproduced in several independent experiments, though the maximal intensity was different from run to run. Although the precise origin of such enhanced fluorescence in 86 mM NaCl solution is currently unknown, we speculate that it can be related to dissociation of RB aggregates (dimers, trimers, etc.) in a salt environment. In contrast to the enhanced fluorescence in a salt environment, we observed quite negligible differences between spectra 1 and 3. This strongly suggests that the effect of the low-molecular

Table 1
Effect of ssDNA on RB fluorescence.

Sample	ssDNA concentration (μM)	RB concentration (μM)	Fl. intensity normalized to reference sample 1
1	0	1.5	1
2	0.3	1.5	0.98
3	1	1.5	0.95

weight components of the GNP supernatant liquid (citrate ions, etc.) on RB fluorescence was negligible.

It should be noted that curve 2 in Fig. 3 demonstrates the maximum observed difference between the aqueous and the salt-containing solutions of RB. Typically, the maximal difference was in the range of 2–5%, whereas the difference between the maxima of spectra 1 and 2 in Fig. 3 was about 15% at 575 nm. Thus, we can conclude that the probe ssDNA, NaCl salt from the hybridization buffer, and the low-molecular-weight components of GNP solutions did not significantly affect the RB fluorescence spectra. However, the recorded variations of fluorescence in a salt environment could reduce the assay sensitivity and increase the low detection limit (see below).

3.2. Effect of the GNP concentration on the fluorescence spectra of RB

The effect of GNPs on the fluorescence properties of RB has been studied by several authors [38–40]. The fluorescence intensity was shown to be strongly dependent on the GNP size [38], concentration [40], and charge [41].

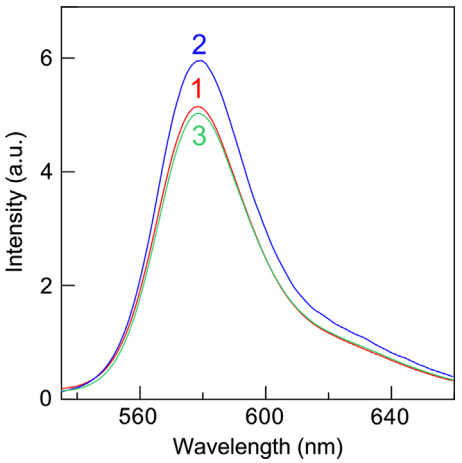

Fig. 3. Fluorescence spectra of RB dissolved in water (1), 86 mM NaCl (2), and GNP supernatant liquid (3).

As RB is a cationic dye [14,41], it can easily be adsorbed on negatively charged citrate GNPs. Depending on the GNP–RB composition, one can observe fluorescence enhancement by GNPs [38–41] or quenching of fluorescent molecules located near metal nanoparticles [34,42].

The fluorescence quenching by GNPs is caused by an increased nonradiative rate and a drastic decrease in the dye's radiative rate [40,42–44]. By contrast to the fluorescence enhancement experiments with GNP films [38–41], fluorescence quenching is usually observed for diluted colloids [19]. In particular, the experimental data of Zhang et al. [14] show that at a GNP concentration of 6.9 nM and an RB concentration of 1.4 μM, strong quenching of RB by GNPs was observed at a moderate ratio of about 200 RB molecules per one 15-nm gold particle. However, the fluorescence spectra of Zhang et al. [14] were not corrected to the inner filter effect, which can obscure the net GNP quenching. Below we provide a set of experimental data aimed at elucidating the GNP concentration effect on fluorescence quenching with the inner filter correction being taken into account.

Fig. 4a shows relative fluorescence intensity as a function of the GNP concentration. Experimental curve 1 was obtained at 575 nm and a constant RB concentration of 1.5 μM with a 1-cm cuvette and an AvaSpec-2048 instrument. The GNP concentrations $N = 3.8 \times 10^{12} A_{520}$ (particles/mL) were found from the optical densities A_{520} of GNP solutions at 520 nm and from the integral extinction cross-section calculated by Mie theory [45].

Curve 1 in Fig. 4a represents uncorrected experimental measurements, whereas curve 2 was corrected to the inner filter effect according to the following approximate equation [34]:

$$I_{corr} = 10^{(A_{520}+A_{575})/2} I_{\exp}, \quad (1)$$

where A_{520} and A_{575} are the optical densities at the excitation and emission wavelengths. Eq. (1) accounts for the absorption of exciting light, which travels to the cuvette's center, and emitted light, which travels from the cuvette's center to the detector. In other words, both geometrical passes within the cuvette are assumed to equal $l/2$ (see the insets in Fig. 4). Actually, the inner filter

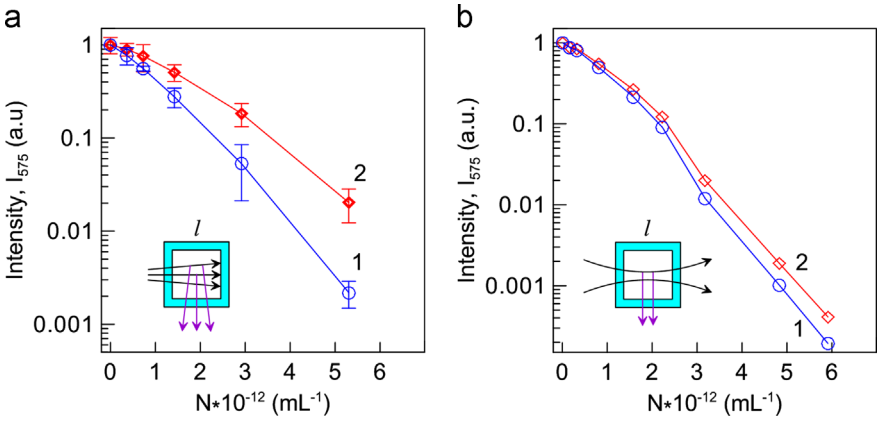

Fig. 4. Fluorescence intensity as a function of the GNP concentration. Curves 1 and 2 represent the experimental (uncorrected) and corrected data, respectively. All measurements were performed with a 1-cm cuvette and an AvaSpec-2048 (a) and a Perkin-Elmer LS-55 (b) instrument. The insets show the corresponding measuring schemes.

effect is manifested as the difference between the measured and the corrected curves. The course of corrected curve 2 can be explained by an increased amount of RB molecules adsorbed on GNPs and their quenching.

At high GNP concentrations (e.g., 6.9 nM, used by Zhang et al. [14]), the difference between the measured and the corrected intensities can be of about one order. However, the actual inner filter correction depends strongly on particular instrument geometry. For example, Eq. (1) only holds for a thin parallel or focused exciting beam and for a detector with a zero viewing angle. As the AvaSpec-2048 instrument does not meet these requirements, we also performed similar measurements with a Perkin-Elmer LS-55 spectrofluorimeter (Fig. 4b). It is evident that this instrument was more suitable for our systems containing GNPs and RB with overlapping absorption bands. In any case, the inner filter effect was reduced significantly as compared with that shown in panel (a). On the other hand, to make the inner filter effect more evident, we used the AvaSpec-2048 instrument in preference to the Perkin-Elmer LS-55 spectrofluorimeter.

The next experiments were done with the same samples as in Fig. 4a but now with the addition of NaCl to initiate aggregation of GNPs (Fig. 5). In these experiments, NaCl was added to an aqueous solution containing 1.5 μM RB and GNPs; the final NaCl concentration was equal to that used for hybridization conditions, 86 mM (Fig. 5b). In a sense, such colloids imitate the spectral properties of DNA-containing systems formed during the hybridization process [11,14]. Actually, the left panel in Fig. 5a reproduces the plots in Fig. 4a, measured with the AvaSpec-2048 instrument. The addition of the salt led to a drastic change in the colloid spectra and, accordingly, to significant differences between the measured intensities for nonaggregated and aggregated systems (compare curves 1 in Fig. 5a and b, respectively). This means that the measured fluorescence intensity can be greatly distorted owing to GNP aggregation, as compared with a nonaggregated colloid. However, it would be erroneous to explain these differences between curves 1 by the net reduction in quenching. Indeed, only the difference between the corrected intensities (i.e., between curves 2 in Fig. 5a and b) can be attributed to a significant reduction in fluorescence quenching by aggregated GNPs. Experimentally, this effect was observed as enhanced fluorescence after the salt addition. Similar results were obtained with the Perkin-Elmer LS-55 instrument (data not shown), although the absolute variations in the intensity of the corrected and noncorrected curves vs the GNP concentration differ from those shown in Fig. 5.

3.3. Correlation between the adsorption of RB molecules on GNPs and the fluorescence intensity

Solutions with a constant final RB concentration (1.5 μM) were incubated with GNP colloids of concentrations ranging from 0 to 5.2×10^{12} particles/mL for 30 min. Then, the mixtures were centrifuged at 10,000*g* for 30 min and the fluorescence intensities of the supernatant liquids I_s were measured at 575 nm. Fig. 6 shows the experimental scheme used to measure the RB adsorption curves in terms of the ratios I_s/I_0 and $(I_s-I_0)/I_0$, where I_0 is the fluorescence intensity of a reference aqueous RB solution at 575 nm. CF stands for centrifugation of samples after 30-min incubation. In a sense, the $(I_s-I_0)/I_0$ plots in Fig. 6 can be considered to be an adsorption isotherm for RB molecules adsorbing on GNPs. Indeed, the difference between I_s and I_0 correlates with the amount of RB molecules adsorbed on GNPs; therefore, the ratio $(I_s-I_0)/I_0$ is proportional to the fraction of adsorbed RB molecules. With an increase in the amount of added GNPs, the fraction of adsorbed molecules should increase from 0 to 1, provided that the adsorption is not reversible. Owing to the fluorescence quenching of the adsorbed RB, the ratio I_s/I_0 should decrease from 1 (the initial RB solution without GNPs) to 0 (complete adsorption and quenching of RB on GNPs).

It follows from Fig. 6 that RB molecules are practically absent from the supernatant liquids obtained for colloids with the maximal GNP concentration. In addition, Fig. 4 shows negligible fluorescence for the RB+GNPs systems at the same maximal GNP concentrations. Therefore, these experiments give unambiguous evidence for a direct correlation between complete disappearance of fluorescence and complete adsorption of all RB molecules on the GNPs, as it follows from our measurements of the supernatant liquids. Consequently, at the maximal GNP concentration (about

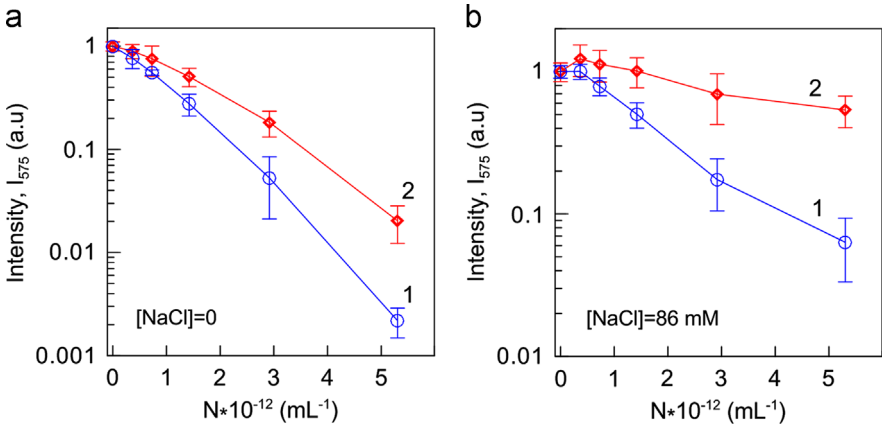

Fig. 5. Fluorescence intensity as a function of the GNP concentration, as measured for NaCl concentrations of 0 (a) and 86 mM (b). For details, see the text.

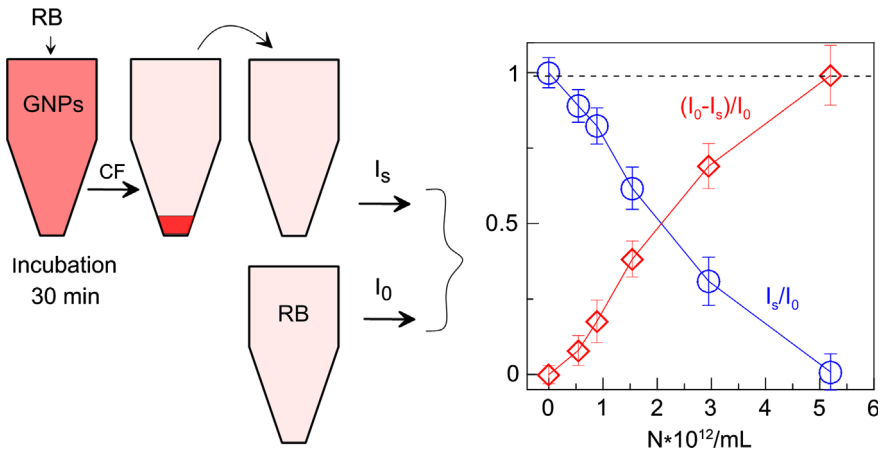

Fig. 6. Experimental scheme for measuring the adsorption of RB molecules on the GNP surface. The plots on the right show the relative intensities I_s/I_0 and $(I_s-I_0)/I_0$ vs the GNP concentration.

Table 2
The relative changes δA and δI for six samples consisting of RB molecules, bare GNPs, or GNPs preincubated with ssDNA. For details, see the text.

No.	Sample	$N \times 10^{12}$ mL^{-1}	A_{520}	δA (%)	I/I_0 (a.u.)	δI (%)
1	GNP+RB	2.8	0.79	0	0.42	0
2	GNP+300 nM ssDNA+RB	2.8	0.83	5.1	0.35	−17
3	GNP+1 μM ssDNA+RB	2.8	0.85	7.6	0.38	−9.5
4	GNP+RB	5.1	1.40	0	0.033	0
5	GNP+300 nM ssDNA+RB	5.1	1.43	2.1	0.035	+6.3
6	GNP+1 μM ssDNA+RB	5.1	1.39	−0.7	0.027	−21

5×10^{12} mL^{-1}), fluorescence was completely quenched owing to the adsorption of RB on metal particles rather than owing to the inner filter effect. It is obvious that this quenching mechanism plays a crucial role in the fluorescence assay based on DNA induced aggregation of GNPs in solutions containing RB molecules.

3.4. Quenching of RB fluorescence by GNP+ssDNA complexes

In Section 3.1, we have shown that the dissolved ssDNA molecules did not affect the RB fluorescence intensity. However, the adsorption of RB on bare GNPs resulted in quenching of RB fluorescence (Sections 3.2 and 3.3). In this section, we examine whether the ssDNA being adsorbed on a GNP can interact with RB and can influence RB quenching. In other words, we here examine whether RB molecules can be quenched by GNP+ssDNA complexes in the same manner as they can be quenched by bare GNPs.

Table 2 lists the optical densities and the relative fluorescence intensities for six samples consisting of RB molecules, bare GNPs, or GNPs preincubated with ssDNA. In all experiments, the RB concentration was kept constant (1.5 μM), whereas the GNP concentration was equal to 2.8×10^{12} mL^{-1} (for the first three samples) and 5.1×10^{12} mL^{-1} (for the other three samples). Two concentrations of ssDNA were tested: 300 nM and 1 μM. In all cases, the GNP+RB systems were used as reference fluorescent samples. I_0 is the intensity of an aqueous RB solution.

It follows from the data of Table 2 that the optical densities of the GNP+ssDNA complexes after the addition of RB molecules do not differ significantly from the optical densities of the reference solutions. The fluorescence intensity variations were higher than the variations in optical densities. The initial fluorescence intensity of RB solutions without bare GNPs or GNP+ssDNA complexes was equal to 57 a.u.—about 30 times higher than that for fluorescence intensities of the last three samples. Therefore, we conclude that almost complete quenching of RB had occurred for all the samples.

From these experiments, we conclude that the interaction between GNPs and ssDNA does not change significantly the RB quenching and should not interfere with the DNA fluorescence test.

3.5. Enhancement of RB fluorescence by GNPs at low GNP concentrations

According to the model proposed by Gersten and Nitzan [46], there are two mechanisms of fluorescence enhancement related to the enhancement of the local field near a nanoparticle at the excitation wavelength and to the change in the partitioning of the excitation energy. In the case of GNPs, the field enhancement is induced by excited localized surface plasmons, whereas the second mechanism comes from modification of decay channels by the plasmonic nanoparticle [39,42]. It should be emphasized that the plasmonic enhancement of fluorescence has been observed for specific experimental conditions [38–41] at very high RB/GNP molar ratio and for negatively charged particles only [41].

Here, we describe our observation of GNP-enhanced RB fluorescence in the case of low GNP concentrations and a low RB/GNP molar ratio. The enhanced fluorescence was recorded at a constant RB concentration of 1.5 μM and for GNP concentrations below 10^{12} particles/mL with a Perkin-Elmer LS-55 instrument equipped with a 3-mm glass cuvette. The measurements were made at 2 and 24 h after mixing of RB and GNP solutions. In general, the measured intensities were similar for both experimental

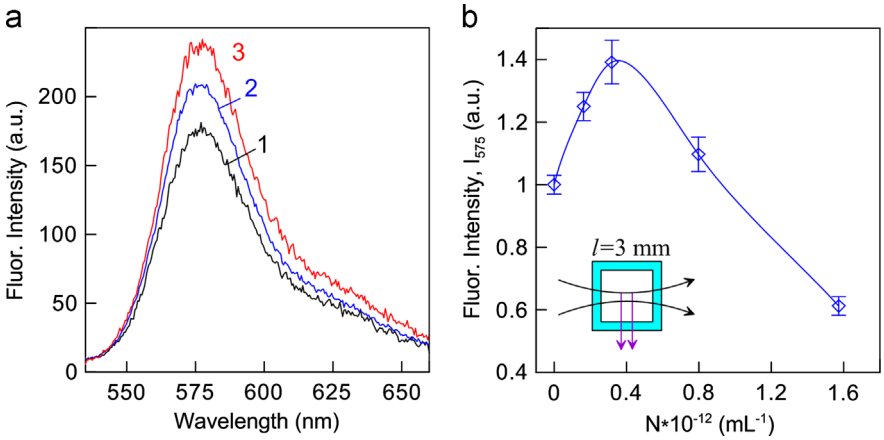

Fig. 7. (a) Fluorescence spectra of aqueous mixtures containing a constant concentration of RB (1.5 μM) and different concentrations of GNPs [0 (1), 1.6×10^{12} (2), and 3.2×10^{12} (3) particles/mL]. Note that fluorescence intensity increased with increasing concentration of GNPs. (b) Dependence of the fluorescence maxima I_{575} on the GNP concentration. This plot illustrates the existence of an optimal GNP concentration (about 0.4×10^{12} particles/mL) for fluorescence enhancement.

set of observations, so the spectra were averaged over a 2- and a 24-h incubation time.

Fig. 7 shows the averaged fluorescence spectra of aqueous mixtures of RB and GNPs and the dependence of the intensity maxima I_{575} on the GNP concentration. All the measurements were done in a 3-mm cuvette with a Perkin-Elmer LS-55 instrument. In general, the concentration dependence in panel (b) resembles that reported by Levchenko et al. [41] for 13.6-nm GNP size, which is close to the size of our GNPs. However, their RB (50 μM)/GNP (4 μM)=12.5 M ratio was almost 250 times higher than our ratio RB (1.5 μM)/GNP (30 μM)=0.05. Zhu et al. [40] also reported a concentration-dependent fluorescence enhancement by GNPs with a maximum near the GNP concentration of 14 μM. Again, their RB/GNP molar ratio was about 5, almost two orders higher than our RB/GNP ratio of 0.05. Moreover, Zhu et al. [40] used 40-nm GNPs; therefore, we had to compare the numbers of molecules per unit GNP surface rather than the molar ratios. As the specific surface of a colloid scales inversely with the particle size at a constant molar or mass/volume concentration, the number of RB molecules per unit GNP surface in our case was almost three orders lower. In their explanation of the GNP-induced fluorescence enhancement, Zhu et al. [40] used a model for an RB-capped gold nanosphere to calculate the local electrostatic filed enhancement. As any optically dense dielectric shell shifts the plasmon resonance to longer wavelengths [47], the local field factor first increases and then decreases.

The exact reasons for the recorded nonmonotonic dependence in Fig. 7b are currently unknown, because the model [40] hardly holds in our case. The electromagnetic mechanism of enhancement seems doubtful, because we observed fluorescence quenching for an increasing GNP concentration, even after the inner filter correction. Another possible explanation is an inverted inner filter effect, caused by a red-shifted GNP extinction spectrum, which, in turn, results in an increased beam intensity at the excitation wavelength. In any case, the small size of our particles is not optimal for observation of a significant enhancement of fluorescence. For example, Nakamura and Hayashi [38] found a size-dependent enhancement with an optimum near 150 nm. As the high RB/GNP molar ratio is not suitable for DNA detection based on a GNP-induced quenching mechanism, we did not investigate GNP-enhanced fluorescence in detail. This important question is beyond the scope of this work and deserves further study.

3.6. *DNA detection assay based on fluorescence quenching of Rhodamine B by GNPs*

Zhang et al. [14] performed a thorough optimization of the DNA detection assay with regard to NaCl, probe DNA, and target cDNA conditions. Therefore, our experimental conditions for DNA detection and the assay protocol were the same as those used in [14]. However, in contrast to the data of Zhang et al. [14], we observed rather worse reproducibility of assay results and, accordingly, our detection limit was significantly higher than that reported in [14].

The top row in Fig. 8 shows the colors of tubes with GNPs mixed with solutions of ssDNA (tube 8; noncomplementary target, 300 nM), with dsDNA after hybridization of the probe and target DNA (tubes 1–7; target cDNA concentrations, 300, 30, 3, 0.3, 0.03, 0.003, and 0.0003 nM), and finally with the detection buffer and RB solution (tube 9). Other reaction conditions are as follows: GNP concentration, 5.3×10^{12} mL^{-1}; concentration of probe ssDNA in hybridization buffer, 300 nM; and RB concentration, 1.5 μM.

The bottom row shows the same samples irradiated with a UV flatbed fluorescence detector. For the left top sample with the highest concentration of the target cDNA (300 nM), the solution color changed from red to purple, indicating the aggregation of GNPs. In the bottom row, this left tube fluoresced most intensely, although this difference from other fluorescent tubes is quite small for the naked eye. Therefore, because of the small changes in the color of the top-row colloids and in the fluorescent intensities of the bottom-row tubes, we cannot expect that the method will be highly sensitive below nanomolar cDNA

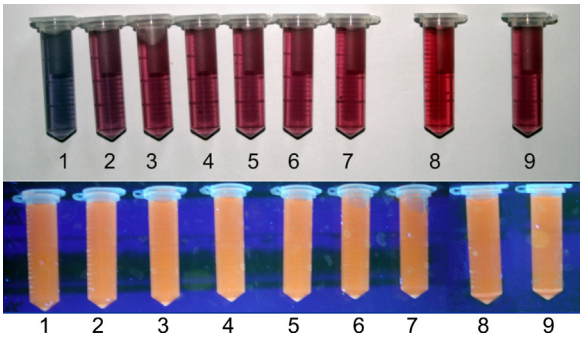

Fig. 8. Photos of the samples under visible (top) and UV (bottom) light illumination. For details, see the text. (For interpretation of references to color in this figure, the reader is referred to the web version of this article.)

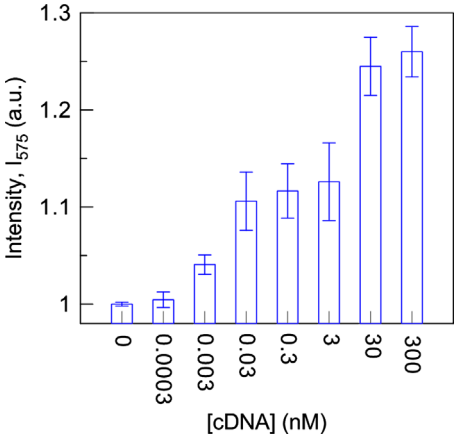

Fig. 9. Dependence of the RB fluorescence intensity on the concentration of the target cDNA.

concentrations. Indeed, our measurements of the fluorescence intensities for samples 1–7 and 9 (Fig. 9) demonstrate only a 30% difference in the fluorescent intensities between samples 1 and 9, whereas the differences in colors of the same samples are evident to the naked eye.

In agreement with Zhang et al.'s [14] findings, Fig. 9 shows a nonlinear relationship between the cDNA concentration and the fluorescence intensity (note that the abscissa scale is logarithmic). Because of random variations, the difference between the intensities for the blank sample ([cDNA]=0) and for the minimal cDNA concentration (0.3 pM) is not statistically significant on the level of two mean square errors. Furthermore, increasing the cDNA concentration from 0.3 pM to 0.3 nM led to quite a small, 10% increase in the fluorescence intensity. Taking into account the typical experimental errors, we estimate a realistic low detection limit (LDL) to be in the range 30–100 pM. This finding is in agreement with the previously reported 100 pM LDL for the colorimetric assay [48] and 10 pM LDL for the dynamic light scattering assay [10,11]; however, it disagrees with the result of Zhang et al. (0.29 pM LDL [14]).

4. Conclusions

We have studied the optical mechanisms underlying the DNA detection assay based on fluorescence quenching of the fluorescent dye Rhodamine B by GNPs. The assay principle is based on the different ability of single- and double-stranded DNA to stabilize GNPs in a salt environment. In the first set of experiments, we have shown that the probe ssDNA and the low-molecular components of GNP solutions do not affect the RB fluorescence spectra, although we have observed notable variations in the spectra for different NaCl concentrations, in agreement with previous observations [14].

In Section 3.3, we have examined the fluorescence of GNP+RB supernatant liquids and we have provided an unambiguous proof for a direct correlation between complete fluorescence quenching and complete adsorption of all RB molecules on GNPs. Our main result is that both the inner filter effect and the quenching of the dye owing to its adsorption on GNPs contribute to the DNA detection assay based on measurements of fluorescence in mixtures of GNPs, ssDNA, dsDNA, and the RB dye. Finally, according to our estimates, the LDL of the fluorescent DNA assay lies in the range 30–100 pM, which is close to the LDLs reported previously for DNA assays based on extinction spectra and on static and dynamic light scattering measurements.

Acknowledgments

This research was supported by grants of the Russian Foundation for Basic Research (Nos. 12-04-00629-a, 12-02-00379-a, and 11-02-00128-a); the Programs of the Presidium of the Russian Academy of Sciences “Basic Sciences for Medicine” and “Basic Technologies for Nanostructures and Nanomaterials”; and the Government of the Russian Federation (a grant to support scientific research projects implemented under the supervision of leading scientists at Russian institutions of higher education). P.T.E. was supported by a U.M.N.I.K. grant from the Bortnik Foundation. We thank Mr. D.N. Tychinin (IBPPM RAS) for his help in preparation of the manuscript.

References

[1] Mullis KB, Faloona FA. Specific synthesis of DNA in vitro via a polymerase-catalyzed chain reaction. Methods Enzymol 1987;155:335–50.
[2] Espy MJ, Uhl JR, Sloan LM, Buckwalter SP, Jones MF, Vetter EA, et al. Real-time PCR in clinical microbiology: applications for routine laboratory testing. Clin Microbiol Rev 2002;19:165–256.
[3] Mirkin CA, Letsinger RL, Mucic RC, Storhoff JJ. A DNA-based method for rationally assembling nanoparticles into macroscopic materials. Nature 1996;382:607–9.
[4] Park HG. Nanoparticle-based detection technology for DNA analysis. Biotechnol Bioprocess Eng 2003;8:221–6.
[5] Elghanian R, Storhoff JJ, Mucic RC, Letsinger RL, Mirkin CA. Selective colorimetric detection of polynucleotides based on the distance-dependent optical properties of gold nanoparticles. Science 1997;277:1078–81.
[6] Katz E, Willner I. Integrated nanoparticle–biomolecule hybrid systems: synthesis, properties, and applications. Angew Chem Int Ed, 43; 6042–108.
[7] Nam JM, Thaxton CS, Mirkin CA. Nanoparticle-based bio-bar codes for the ultrasensitive detection of proteins. Science 2003;301:1884–6.
[8] Rosi NL, Mirkin CA. Nanostructures in biodiagnostics. Chem Rev 2005;105:1547–62.
[9] Sato K, Hosokawa K, Maeda M. Rapid aggregation of gold nanoparticles induced by non-cross-linking DNA hybridization. J Am Chem Soc 2003;125:8102–3.

[10] Dai Q, Liu X, Coutts J, Austin L, Huo Q. A one-step highly sensitive method for DNA detection using dynamic light scattering. J Am Chem Soc 2008;130:8138–9.
[11] Pylaev TE, Khanadeev VA, Khlebtsov BN, Dykman LA, Bogatyrev VA, Khlebtsov NG. Colorimetric and dynamic light scattering detection of DNA sequences by using positively charged gold nanospheres: a comparative study with gold nanorods. Nanotechnology 2011;22: 285501. (11 pp.).
[12] Maxwell DJ, Taylor JR, Nie S. Self-assembled nanoparticle probes for recognition and detection of biomolecules. J Am Chem Soc 2002;124:9606–12.
[13] Li H, Rothberg L. DNA sequence detection using selective fluorescence quenching of tagged oligonucleotide probes by gold nanoparticles. Anal Chem 2004;76:5414–7.
[14] Zhang H, Wang L, Jiang W. Label free DNA detection based on gold nanoparticles quenching fluorescence of Rhodamine B. Talanta 2011;85:725–9.
[15] Li H, Rothberg LJ. Label-free colorimetric detection of specific sequences in genomic DNA amplified by polymerase chain reaction. J Am Chem Soc 2004;126:10958–61.
[16] Li H, Rothberg LJ. Colorimetric detection of DNA sequences based on electrostatic interactions with unmodified gold nanoparticles. Proc Natl Acad USA 2004;101:14036–9.
[17] Anger Pascal, Bharadwaj Palash, Novotny Lukas. Enhancement and quenching of single-molecule fluorescence. Phys Rev Lett 2006;96: 113002.
[18] Kühn S, Håkanson U, Rogobete L, Sandoghdar V. Enhancement of single-molecule fluorescence using a gold nanoparticle as an optical nanoantenna. Phys Rev Lett 2006;97:017402.
[19] Lakowicz JR. Radiative decay engineering 5: metal-enhanced fluorescence and plasmon emission. Anal Biochem 2005;337:171–94.
[20] Liaw J-W, Chen C-S, Chen J-H. Enhancement or quenching effect of metallic nanodimer on spontaneous emission. J Quant Spectrosc Radiat Transfer 2010;111:454–65.
[21] Gersten J, Nitzan A. Electromagnetic theory of enhanced Raman-scattering by molecules adsorbed on rough surfaces. J Chem Phys 1980;73:3023–37.
[22] Schatz GC, Young MA, Van Duyne RC. Electromagnetic mechanism of SERS. In: Kneipp K, Moskovits M, Kneipp H, editors. Surface-enhanced Raman scattering—physics and applications, Topics in applied physics, 103. Berlin: Springer; 2006. p. 19–46.
[23] Le Ru EC, Etchegoin PG. Principles of surface—enhanced Raman spectroscopy and related plasmonic effects. Amsterdam: Elsevier; 2009.
[24] Stockman MI. Nanoplasmonics: past, present, and glimpse into future. Opt Exp 2011;19:22029–106.
[25] Le Ru EC, Grand J, Sow I, Somerville WRC, Etchegoin PG, Mona Treguer-Delapierre M, et al. A scheme for detecting every single target molecule with surface-enhanced Raman spectroscopy. Nano Lett 2011;11:5013–9.
[26] Thomas M, Greffet J-J, Carminati R, Arias-Gonzalez JR. Single-molecule spontaneous emission close to absorbing nanostructures. Appl Phys Lett 2004;85:3863–5.
[27] Pelton M, Aizpurua J, Bryant G. Metal-nanoparticle plasmonics. Laser Photonics Rev 2008;2:136–59.
[28] Bardhan R, Grady NK, Cole JR, Joshi A, Halas NJ. Fluorescence enhancement by au nanostructures: nanoshells and nanorods. ACS Nano 2009;3:744–52.
[29] Khlebtsov NG, Melnikov AG, Dykman LA, Bogatyrev VA. Optical properties and biomedical applications of nanostructures based on gold and silver bioconjugates. In: Videen G, Yatskiv YS, Mishchenko MI, editors. Photopolarimetry in remote sensing. Dordrecht: Kluwer Academic Publishers; 2004. p. 265–308.
[30] Khlebtsov NG. *T*-matrix method in plasmonics: an overview. J Quant Spectrosc Radiat Transfer 2011;123:184–217.
[31] Rechberger W, Hohenau A, Leitner A, Krenn JR, Lamprecht B, Aussenegg FR. Optical properties of two interacting gold nanoparticles. Opt Commun 2003;220:137–41.
[32] Khlebtsov BN, Melnikov AG, Zharov VP, Khlebtsov NG. Absorption and scattering of light by a dimer of metal nanospheres: comparison of dipole and multipole approaches. Nanotechnology 2006;17: 1437–45.
[33] Khlebtsov BN, Zharov VP, Melnikov AG, Tuchin VV, Khlebtsov NG. Optical amplification of photothermal therapy with gold nanoparticles and nanoclusters. Nanotechnology 2006;17:5167–79.
[34] Lakowicz JR. Principles of fluorescence spectroscopy. 2nd ed. New York; 1999.
[35] Frens G. Controlled nucleation for the regulation of the particle size in monodisperse gold suspensions. Nature Phys Sci 1973;241:20–2.
[36] Grabar KC, Freeman RG, Hommer MB, Natan MJ. Preparation and characterization of Au colloid monolayers. Anal Chem 1995;67: 735–43.
[37] Khlebtsov NG, Bogatyrev VA, Dykman LA, Melnikov AG. Spectral extinction of colloidal gold and its biospecific conjugates. J Colloids Interface Sci 1996;180:436–45.
[38] Nakamura T, Hayashi S. Enhancement of dye fluorescence by gold nanoparticles: analysis of particle size dependence. Jpn J Appl Phys 2005;44:6833–7.
[39] Sen T, Sadhu S, Patra A. Surface energy transfer from rhodamine 6G to gold nanoparticles: a spectroscopic ruler. Appl Phys Lett 2007;91: 043104–6.
[40] Zhu J, Zhu K, Huang L-q. Using gold colloid nanoparticles to modulate the surface enhanced fluorescence of Rhodamine B. Phys Lett A 2008;372:3283–8.
[41] Levchenko V, Grouchko M, Magdassi S, Saraidarov T, Reisfeld R. Enhancement of luminescence of Rhodamine B by gold nanoparticles in thin films on glass for active optical materials applications. Opt Mater 2011;34:360–4.
[42] Anger P, Bharadwaj P, Novotny L. Enhancement and quenching of single-molecule fluorescence. Phys Rev Lett 2006;96:113002.
[43] Cannone F, Chirico G, Bizzarri AR, Cannistraro S. Quenching and blinking of fluorescence of a single dye molecule bound to gold nanoparticles. J Phys Chem B 2006;110:16491–8.
[44] Aslan K, Perez-Luna VH. Quenched emission of fluorescence by ligand functionalized gold nanoparticles. J Fluoresc 2004;14:401–5.
[45] Mie G. Beiträge zur Optik trüber Medien, speziell kolloidaler Metallösungen. Ann Phys 1908;25:377–445.
[46] Gersten J, Nitzan A. Spectroscopic properties of molecules interacting with small dielectric particles. J Chem Phys 1981;75:1139–52.
[47] Khlebtsov NG. Optical models for conjugates of gold and silver nanoparticles with biomacromolecules. J Quant Spectrosc Radiat Transfer 2004;89:143–53.
[48] He W, Huang CZ, Li YF, Xie JP, Yang RG, Zhou PF, et al. One-step label-free optical genosensing system for sequence-specific DNA related to the human immunodeficiency virus based on the measurements of light scattering signals of gold nanorods. Anal Chem 2008;80:8424–30.